BUOYANCY VORTEX POWER FROM LOW-TEMPERATURE HEAT

Neil Hawkes [1*], Richard Flay [1], John Cater [2]

[1]Mechanical Engineering, University of Auckland, Auckland, New Zealand

[2] Engineering Science, University of Auckland, Auckland, New Zealand

nhaw121@aucklanduni.ac.nz

Keywords: *Power generation, waste heat, low temperature, buoyancy vortices, vortex.*

ABSTRACT

A modification of the heat-engine theory of Renno and Bluestein (2001) is proposed for an improved prediction of vortex height, thermodynamic efficiency and tangential velocity in atmospheric buoyancy vortices, through a reconsideration of the cold reservoir of the heat engine, as occurring in a turbulent plume above the vortex core. Preliminary modeling suggests a carbon-neutral method of converting energy from waste heat at temperatures below 60℃ to electricity with an efficiency of the order of 5% by exploiting saturated convection.

NOMENCLATURE

C_p	Specific heat of air at constant pressure [J/kgK]
C_w	Specific heat of water [J/kgK]
g	Acceleration due to gravity [m/s^2]
h	Height of the unstable layer [m]
H	Height of the super-adiabatic layer [m]
L_v	Specific latent heat of vaporisation of water [J/kgK]
ΔLR	Lapse rate divergence [℃/km]
Δp	Pressure difference [Pa]
p_∞	Pressure at infinite radius at ground level [Pa]
r	Mixing ratio [g/kg]
r_a	Radius [m]
R	Gas constant for air [J/kgK]
T	Absolute temperature [K]
$\overline{T_s}$	Entropy averaged temperature of heating [K]
T_m	Average temperature of the unstable layer [K]
ΔT	Horizontal temperature difference, core to environment [℃]
V	Velocity [m/s]
$\sqrt{x}$	Non-dimensionalizing vortex radius [s$^{1/2}$]
β	Atmospheric instability [s^{-1}]
γ	Friction efficiency – the fraction of the total frictional energy dissipated at the ground
Γ	Circulation [m^2/s]
Γ_∞	Environmental circulation at infinite radius
η	Carnot efficiency
ν	Kinematic viscosity [m^2/s]
w	Axial (vertical) velocity [m/s]
$'$	Denotes differentiation with respect to height

1. INTRODUCTION

Many attempts have been made to exploit waste heat for electrical power generation, but the low power densities available at low temperatures make the equipment required for such a process impractically large and expensive [1]. For "fuel-free" energy sources, capital and operating costs are key to economic viability. Using an atmospheric buoyancy vortex (a whirlwind akin to a dust-devil or waterspout) for power generation through converting waste heat into kinetic energy in the vortex and then into electricity (hereafter referred to as Buoyancy Vortex Power or BVP) is appealing since tall structures and large turbines can be avoided. The vortex may be very tall but can be produced cheaply using a BVP vortex station of the type we propose.

The swirl in these rising hot-air flows suppresses turbulent mixing so that more energy from buoyancy is available as kinetic energy at the ground than that seen at the base of a turbulent plume [2, 3]. These high energy flows can drive a small, high-speed wind turbine at ground level. Other authors have considered BVP but have not determined the circumstances needed for sufficiently strong vortices to form. Review papers [4, 5] discuss the variety of methods for extracting power from vortices that have been proposed but do not address this question directly.

We suggest that strong vortices must be tall. For this to occur in small diameter vortices, lapse rate divergence must be available, to increase the aspect ratio of the vortex.

Lapse rate is the rate of temperature drop in rising through the atmosphere [℃/km]. Lapse rate divergence is the degree to which the core flows cool more slowly than the surroundings in rising.

2. BUOYANCY VORTICES

Natural buoyancy vortices occurring in the atmosphere require buoyancy and concentrated horizontal rotation around a vertical axis or "swirl." Swirl arises from the turning of horizontal vorticity, driven by wind shear at the ground, into the vertical axis either by convection [6, 7] or via the end-wall effect (explained below). In the absence of vertical acceleration in the vortex core flows, arising from lapse rate divergence, buoyancy vortex cores display a characteristic aspect ratio (height/diameter) of the order of 10:1 [8]. Mesoscale vortices such as hurricanes will, therefore, extend up to the tropopause, but this is not necessarily so for much smaller vortices.

Dust-devils are dry buoyancy vortices. They do not extend to the top of the convective layer of the atmosphere, although the plumes and thermals above them may do so. Even so, they display aspect ratios much greater than 10:1 [9].

Some waterspouts occur independently of a parent storm. These are the closest natural analog of our proposed BVP vortex, dynamically similar to dust devils but driven by the buoyancy of warm saturated air, cooling at the pseudo-adiabatic lapse rate due to release of latent heat through condensation [10]. In temperate atmospheres, condensation is dominant in driving convection, but in dry deserts, super-adiabatic atmospheric boundary layers develop above the desert floor, allowing tall dust-devils to be driven by dry adiabatic convection [11]. In both cases, we see lapse-rate divergence producing vertical acceleration, axial strain, extended aspect ratios, lower cold reservoir temperatures, higher thermodynamic efficiencies, and stronger vortices.

We propose that a buoyancy vortex can be considered as containing four zones:-

- Core: a cylindrical column with cyclostrophic flows (flows in cyclostrophic balance - where radial pressure gradient balances apparent centrifugal force) in near solid-body-rotation and with positive buoyancy driving an updraft.
- Potential vortex: a larger annulus surrounding the core, with weaker cyclostrophic flows that can be considered as inviscid, irrotational and neutrally buoyant.
- End wall disc: where the potential vortex flows meet the ground and are subject to the end-wall effect. Significant inflow acceleration occurs at the center of the disc.
- Plume: the turbulent plume and thermals formed above the core.

Three simultaneous phenomena are observed in a buoyancy vortex: the End Wall Effect, the Heat Engine, and Core Stability

We suggest the persistence of the vortex core to aspect ratios above 10:1 depends upon the stability of the core modifying turbulent mixing. The height to which the core persists before breakdown to a turbulent plume affects the airflows at the ground since only energy released in the core contributes significantly to driving them. Energy released in the plume is expended in lifting and warming of entrained air [12]. We suggest that the base of the plume should, therefore, be considered as the cold reservoir of the heat-engine driving the vortex flows, to predict vortex strength.

Vortex cores may have a one-cell or two-cell structure depending on swirl strength [13]. This is a different phenomenon from the breakdown to a plume and apparently does not need to be considered to model the heat engine [11].

2.1 End Wall Effect

The term ‘end wall effect’ describes the interaction between a viscous vortex and a surface that is perpendicular to the vortex axis, resulting in flow concentration near the vortex axis. For a buoyancy vortex, friction at the ground and wind shear above it reduce the tangential velocity and the centrifugal force, thus allowing air to be drawn into the vortex base by a radial pressure gradient. The radial pressure gradient arises from the buoyancy of the core [11]. Analysis [14] shows flows from the potential vortex being drawn down and inwards as they approach the ground, due to viscosity.

The streamlines in cross section are predicted for different constants of integration ‘C’ (relating to initial radius in the potential vortex) as shown in figure 1a).

Wind speed at the ground is maximized when a two-cell structure is established immediately above the ground in a ‘drowned vortex jump’ (DVJ) [13]. In a DVJ the corner flows (where the flows turn from horizontal to vertical, as in figure 2) can have twice the speed of the maximum tangential flows in the core [18].

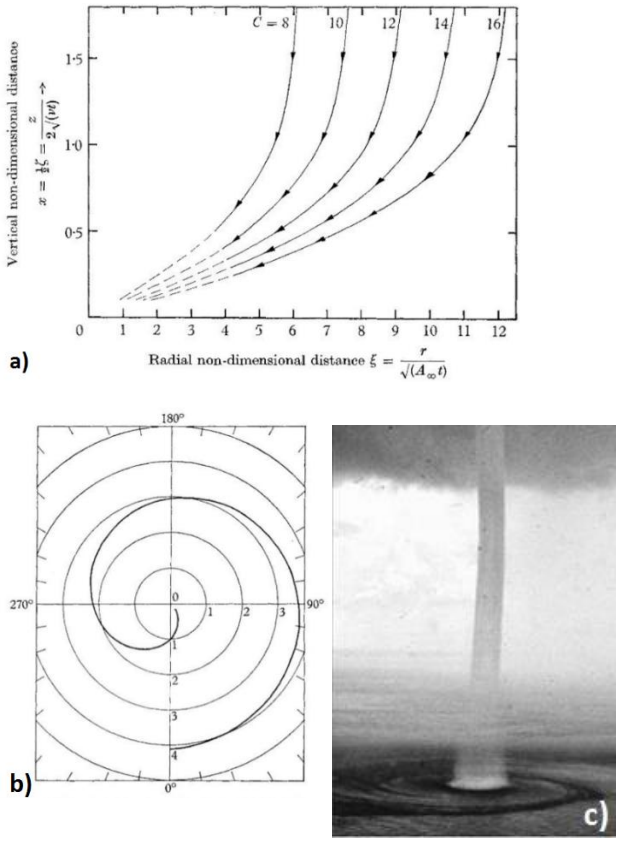

Figure 1. a) Inflow to the base of a columnar vortex induced by viscosity in scaled vertical cross-section, showing inflow streamlines for different constants of integration ‘C’ [14].

b) Inflow streamline in plan [14].

c) Waterspout off the Florida Keys showing inflow similar to (b) made visible on the sea surface and the core made visible by condensation [15].

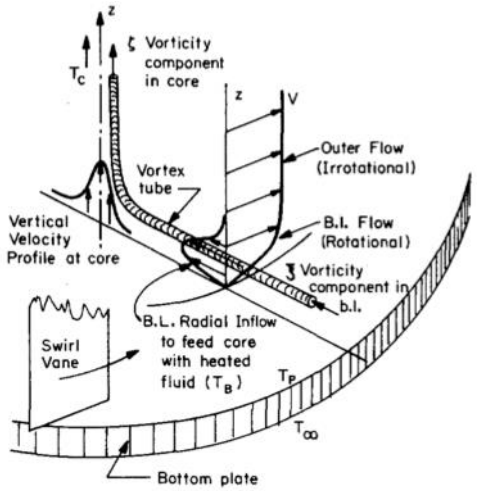

Figure 2. The concentration of vorticity through turning of horizontal vorticity to the vertical [16].

Another way to visualize the end wall effect is given in [16] by considering vortex tubes as shown in figure 2. A vortex tube visualizes vorticity being transported through a fluid along with the flow, with vorticity being aligned to the axis of the tube. LES (Large Eddy Simulation) models have been

made of the flows in the end wall disc and show the flow concentration that results [17, 18].

2.2 Heat Engine

In [11] the authors analyze the thermodynamics of dust-devils. They model them as a heat-engine and consider a dust-devil in quasi-steady state, with work done by the heat engine balanced by mechanical friction. To model the maximum thermodynamic intensity of a vortex in cyclostrophic balance, they assume the cold reservoir is at the average temperature of the convective slab and the hot reservoir is at the temperature at the base of the vortex.

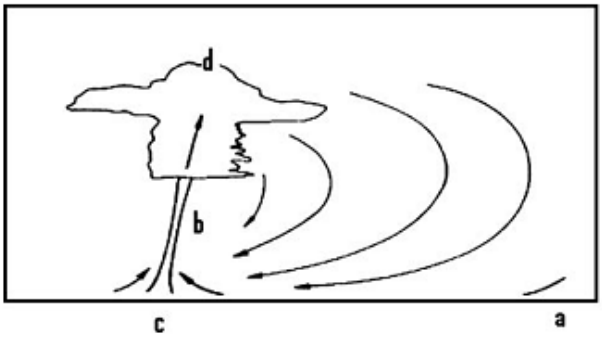

Figure 3. Vortex flows from the ground at (a), to the base at (c), to the core at (b), to the top of the convective slab at (d) [15].

Convectively Available Potential Energy (CAPE) describes the ability of air-parcels with positive buoyancy to do work in rising. The convective slab is the range of heights where CAPE is available. By following an air parcel through the path shown in figure 3, the authors derive relationships for pressure-difference and cyclostrophic-flow-velocities.

The analysis is extended to waterspouts in [10] . Equation 1 is derived for the radial pressure difference arising from core buoyancy:

$$\Delta p \approx p_\infty \left\{1 - \exp\left\{\left(\frac{\gamma\eta}{\gamma\eta-1}\right)\left[\left(\frac{C_p}{R}\right)\left(\frac{T_0-T_\infty}{\bar{T}_s}\right) + \left(\frac{L_v}{R}\right)\left(\frac{r_0-r_\infty}{\bar{T}_s}\right)\right]\right\}\right\} \quad (1)$$

Cyclostrophic balance is assumed, and equation 2 is derived for the maximum tangential velocity in the core using the ideal gas law:

$$V_a = \sqrt{RT_\infty \Delta p / p_\infty} \quad (2)$$

For BVP the implication is that the tangential wind speeds at the base of a vortex can be predicted by analyzing it as a heat engine.

2.3 Core Stability and Turbulent Mixing

The stability of the vortex core modifies turbulent mixing and aids the conversion of CAPE into kinetic energy [2, 3]. This stability in the core arises from two factors: cyclostrophic balance and stable stratification of density. Without that stability, the large velocity gradients in the core would produce rapid turbulent mixing of all quantities, including temperature and vorticity, as seen in a turbulent plume [12, 19].

Different criteria for cyclostrophic stability have been offered [20-22]. In [23] a criterion for core stability was derived that also includes the stable radial gradient of temperature. These criteria for stability consider the threshold for amplification or suppression of a small perturbation. Under a constant supply of turbulent energy, increasing stability moderates the rate of diffusion of momentum [2, 3]. Stability increases with increasing angular momentum and radial temperature gradient but decreases with increased vertical velocity.

The analysis of vortices rising through unstable atmospheres with externally supplied tangential momentum in [24] was originally an axisymmetric model of tornado concentration in saturated air under a rotating storm. A closed set of differential equations for convection and turbulent heat diffusion were produced and similarity solutions of the Navier-Stokes equations derived for two-cell vortices rising in equilibrium through an atmospheric layer with constant lapse-rate divergence. This 'Kuo model' shows vortices adopting an equilibrium described by exponential functions for vertical, radial and tangential velocity and temperature difference and pressure depression, expressed in terms of $\sqrt{x}$ (a scaled radius related to eddy viscosity ν_e) and β (a measure of atmospheric instability).

$$x = \frac{{r_a}^2}{4\nu_e}\,[\mathrm{s}] \quad (3a) \qquad \beta \approx \sqrt{\frac{g}{h}\frac{\Delta T}{T_m}}\,[\mathrm{s}^{-1}] \quad (3b)$$

ΔT is the temperature difference from core to environment at the top of the unstable layer, arising from the lapse rate divergence operating through h. Significant pressure depression occurs inside $\sqrt{x}$ = 6. Maximum tangential velocity occurs at $\sqrt{x}$ = 2. The magnitude of the tangential velocity in [24] is modeled as derived from an external supply of tangential momentum, which is not relevant here.

The expected vortex radius reduces for lower eddy viscosity. The observed radii of most dust-devils are smaller than the Kuo model predicts for values of eddy viscosity seen in other meteorological flows [24, 25], suggesting that turbulent diffusion is reduced in these vortices.

An analysis of vortex intensification and decay was made in [26] based on an asymptotic expansion of the Navier-Stokes equations, non-dimensionalized with respect to an Ekman number. This is a laminar analysis of a one-cell vortex but is claimed to be insensitive to inflow structure. The Ekman number is given by:

$$E = \nu_m / \Gamma_\infty \quad (4)$$

For a vortex to concentrate (tighten and strengthen), the circulation must be large enough to give E<<1 and the product of the area of the updraft and the gradient of average vertical velocity within it must be significantly greater than the molecular kinematic viscosity.

$$Aw' > \nu_m \quad (5)$$

DNS studies [27] have explored the modification of turbulence by rotation, showing a hysteretic transition from 'normal' three-dimensional isotropic turbulence to a quasi-two-dimensional form under increasing rotation. The Rossby number is similar to that holding for the lower wave numbers of the turbulent cascade of scale within a columnar vortex (Ro~1). In a buoyancy vortex, the transition to Q2D turbulence would reduce turbulent diffusion and [24] then predicts a smaller vortex diameter. The reduction of diameter would increase the stable radial temperature gradient, further reinforcing the hysteretic behaviour, so the transition from Q2D to 3D isotropic mixing (where the core breaks down to a plume) will be abrupt.

3. ANALYSIS

If the transition to a turbulent plume is suppressed in the core, then the laminar model of vortex intensification and decay in [26] may be reasonably used in predicting the persistence of the core to height. Using an estimate of the prevailing eddy viscosity (instead of the molecular kinematic viscosity) in equation 5 gives an estimate of the vertical acceleration needed to sustain the core.

Assuming that observed vortex diameters in dust devils are twice the radius of maximum tangential wind in [24], eddy viscosity in the core can be estimated from the observed diameter. If β is used as an estimate of w', the lapse rate required to sustain the core can be estimated. This also requires an estimate of the ratio of updraft radius to core radius. We take a value of 3, assuming the updraft has the radius of the maximum extent of significant pressure depression as modelled in [24].

The estimate is as follows:

- r_a~1.5m as seen in dust-devils in [29] is assumed equivalent to $\sqrt{x}$ = 2 from [24]
- Equation 3a gives eddy viscosity $v_e = 0.14$ m^2/s
- If the radius of updraft is taken as $3r_a$ then equation 5 gives the required gradient of vertical velocity $w' > 2.6\text{x}10^{-3}$ s^{-1}
- Assuming $w' = \beta$, equation 3b then gives the required lapse rate divergence ~0.2℃/km

The eddy viscosity estimate is an order of magnitude below that expected in the atmosphere [24]. The estimate of required lapse rate divergence relies on the relationship between the radius of maximum velocity and the radius of updraft but not on the value of eddy viscosity, as long as the transition to a plume is suppressed.

We propose a simple theory to explain vortex height (before breakdown to a turbulent plume) in atmosphere and consequent wind-speeds at the ground for vortices with diameters of the order of 10 meters, which assumes the core rises upwards while CAPE is positive and lapse rate divergence exceeds 0.2℃/km. Positive vertical acceleration in the core arises from the divergent lapse rates as the rate of release of CAPE increases with height.

$$CAPE(H) \equiv \int_0^H g.\frac{T_{v,parcel}-T_{v,env}}{T_{v,env}}\, dz \text{ [J/kg]} \qquad (6)$$

If H is the height to which sufficient lapse rate divergence is maintained then equation 6 gives the CAPE released in the vortex core [30].

Once there is insufficient lapse rate divergence, the core is assumed to decay to a turbulent plume that takes no part in driving the vortex, beyond acting as a 'buoyant plug' to maintain the pressure difference at the top of the core. The turbulent plume, rather than the convective slab, is therefore taken to form the cold reservoir of the heat engine driving the vortex flows.

The heat engine can then be modeled using equations 1 and 2, using a value for *Tc* at the base of the plume to derive the Carnot efficiency.

3.1 Supporting Evidence from the Literature

3.1.1 Laboratory Experiments

A vortex-generator with adjustable peripheral vanes to generate swirl around a heated plate to induce buoyancy was used in [16]. Temperature profiles were derived for a range of vane angles and power inputs, as seen for example in figure 4, showing a two-cell structure (containing a central downdraft and temperature depression). The form of the temperature profiles and their relationship to the diameter of maximum tangential velocity are similar to the two-cell solution of [24] even though they are not in thermal equilibrium.

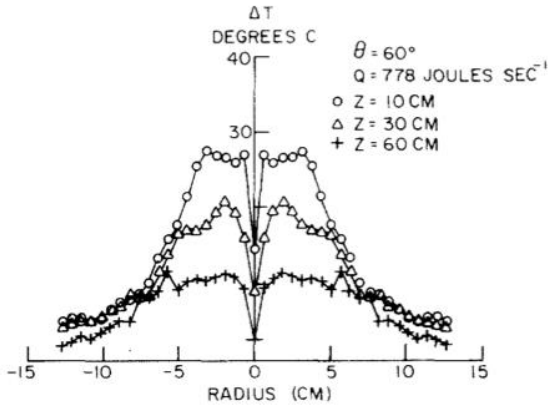

Figure 4. Scaled Temperature excess vs. Radius, 60° vane angle, 778W [16]

Figure 5 shows the rate of decay of maximum temperature difference (scaled to input power) with height for two vortices. The vortices have different power inputs. One is a one-cell vortex and the other a two-cell vortex. They show a common inflection point in their scaled temperature profiles. The scaling of temperature to input power uses established methods in the analysis of turbulent plumes [16].

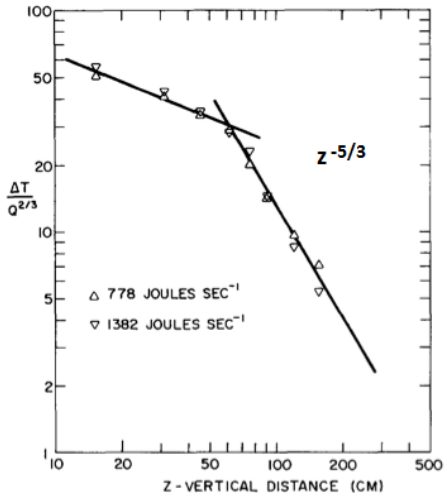

Figure 5. Logarithmic plot of scaled temperature difference vs. height above the base plate showing a $z^{-5/3}$ dependence above the inflexion point [16]

Figure 5 suggests that the temperature difference seen at z=10cm in figure 4 is reduced at greater height by radial diffusion of heat until the core breaks down to a turbulent plume at z=60cm since there is an apparent inflection at that point. Above the inflection, figure 5 shows a $z^{-5/3}$ dependence, which is characteristic of a turbulent plume [12].

The height of the inflection is similar in both vortices and equal to approximately 7 times the core diameter, for the one-cell and two-cell vortices.

Measured circulation strengths given in [16] were used in our earlier paper [31] to give tangential velocity at the outside of the core using equation 7.

$$V_t = \Gamma/\pi d_t \quad (7)$$

Equations 1 and 2 were used to calculate V_a as follows

- Friction efficiency is assumed to be $\gamma = 95\%$ [16]
- Thermodynamic efficiency is $\eta = \frac{T_h - T_c}{T_h}$
- $T_h = T_\infty + \Delta T_h$ and $T_c = T_\infty + \Delta T_c$
- ΔT_c is estimated from figure 5 to be $\Delta T_c = 30 * Q^{2/3}$ to give the cold reservoir temperature at the point of inflection.
- ΔT_h is taken as the maximum temperature at z=10cm for each vortex, or by interpolation between adjacent vortices. For example, $\Delta T_h =$ 28℃ in figure 4.

A linear correlation between modeled and measured tangential velocities (R^2=0.93, sample of 9) was obtained.

Using $\Delta T_c = 0$ (the temperature at the top of the convective layer) would overestimate the velocities observed.

3.1.2 Field Data for Dust Devils

A field study in the Mojave Desert [29] collected data on atmospheric temperature profiles to 1500m and data on passing dust-devils. More detail was made available in a report to NASA on the same field trials [25].

Our analysis of those results [32] using modern software (RAOB) to calculate CAPE and lapse-rates as a function of height, shows that tangential wind speeds measured at the ground suggest dust-devils act as heat engines to convert CAPE(H) (the CAPE released within the super-adiabatic layer) into rotational kinetic energy at an efficiency proportional to the super-adiabatic depth. Resultant tangential velocities from this model (Vm) and measured maximum tangential winds (Vtmax) are shown in figure 6 (R^2=0.82, sample of 71). The results suggest that the lapse rate divergence required to sustain the core is approximately $0.2℃/km$ for core diameters of 1-15m and aspect ratios up to 400:1.

A study of dust-devils in Australia [9] gave statistics for dust-devil height H (equal to the height of the layer of lapse rate divergence in our model) as a percentage of h (the height of the convective layer) which suggests two populations. The upper population shows a mean height H = 51%h, presumably forming in deep super-adiabatic layers formed by winds blowing from adjacent cooler zones. The lower population with a mean height H = 9%h seems to be occurring in the more common super-adiabatic layers formed by strong heating from the ground, similar to those measured in [29].

The temperature of the plumes forming from core break-down at $H \approx 50\%h$ in the upper population will then tend to the mean temperature of the convective layer, which gives estimates of cold reservoir temperature and consequent vortex strength that agree with the upper-bound assumption given in [11]. Variation between individual vortices is also explained.

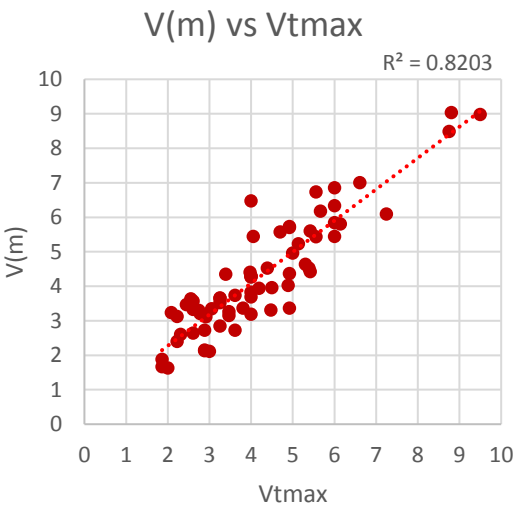

Figure 6. Modelled vs measured maximum tangential velocity in dust-devils [m/s] [32]

For BVP, the implication is that the ability to produce consistent lapse rate divergence to great height in a temperate atmosphere will be crucial in producing strong vortices.

4. VORTEX STATION

A vortex station is proposed using swirl vanes, similar to yacht sails, surrounding a circular concrete pad, to impart swirl to the inflows, as shown in figure 7. Near the center of the pad, hot water is pumped through nozzles at sufficient volume to heat and saturate the air-flow into the vortex core and provide core buoyancy. The majority of the supplied water falls back to the pad after being cooled by evaporation within the DVJ and returns to the source via a central drain. The vortex station thus provides evaporative cooling of waste heat and produces power through BVP.

The innovation compared to other BVP schemes lies in the generation of saturated inflows to produce reliable lapse rate divergence and tall, powerful vortices. This requires pumping through nozzles to produce a 'hot-mist' of finely divided droplets and achieve the required surface area for evaporation and heat transfer in the base of the vortex. Power can be extracted using comparatively small turbines placed in the high wind-speeds occurring in the area of wind concentration in the DVJ.

Such a station may be attractive for retrofit at existing thermal power stations to increase overall station efficiency. If existing station output is limited by warming of river flows, the reduction of heat rejected to the river is also useful.

It may also be used to exploit low-temperature geothermal resources - where the temperature available is too low to raise steam.

The output of a BVP vortex station should be independent of prevailing wind-speeds across a wide range of conditions, relying only on the supply of waste heat, but there will be a maximum wind-speed for stable operation.

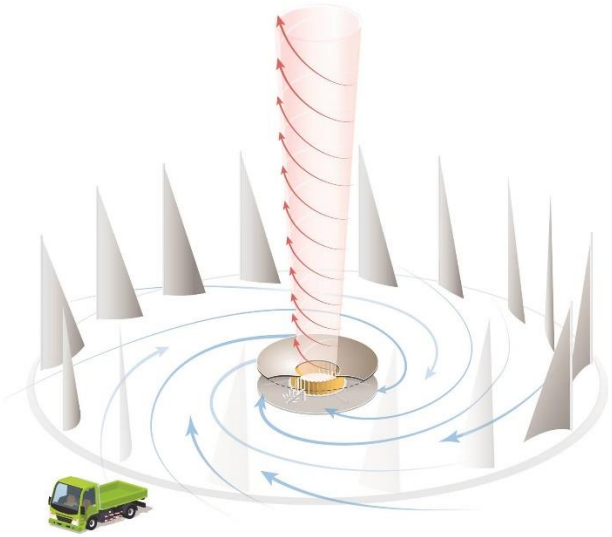

Figure 7. Proposed vortex station schematic (Vortex Power Systems Ltd.)

The DVJ structure can produce wind intensification of approximately two in a vortex of sufficient swirl. A turbine placed in the inflows can produce a radial pressure drop to stabilize the vortex base laterally. The base cannot be blown out of the turbine by a side-wind if the pressure drop across the turbine exceeds the dynamic pressure of the side-wind. For BVP, this suggests that the use of turbines within the area of maximum wind concentration may be more effective than placing turbines in an encircling wall.

Outside of super-adiabatic atmospheric layers in deserts, concentrated buoyancy vortices can only be made with high aspect ratios by using saturated core flows as the source of lapse rate divergence. Dry vortices in neutral atmospheres tend to an aspect ratio of approximately 10:1, with consequent low thermal efficiencies. Saturated air cools more slowly in rising as condensation releases latent heat. If condensate is centrifuged out of the vortex core, the core cooling process should closely follow the pseudo-adiabatic lapse rate. The pseudo-adiabatic lapse rate from a saturated hot reservoir will diverge from the environmental lapse rate up to the tropopause, except under conditions of thermal inversion. Saturated BVP vortices could, therefore, rise high into the atmosphere, until they encounter the tropopause, as shown in figure 8.

Figure 8 is a tephigram: a diagram of temperature varying in the atmosphere, primarily with respect to pressure but also, therefore, with height. The release of CAPE is proportional to the area between the process and environmental traces on the tephigram.

In figure 8 a vortex is fed at the ground with saturated air at $T_h = 40℃$ in a representative NZ summer atmosphere. There is a region of temperature inversion between points A and B on the environmental trace. This is a shallow layer in atmosphere where temperature rises with height – apparently occurring above a cloud layer.

According to the proposed theory the vortex should persist to the tropopause with the core process trace following the pseudo-adiabatic lapse rate to $T_c = 2℃ = 275K$ at 250mbar (H~10km) assuming the vortex can persist through the temperature inversion. The environmental temperature at the tropopause at point C is $-50℃$ at 250mbar, so the temperature difference between the core and the environment has increased from $22℃$ at the ground to $52℃$ at 10km height. The increase in temperature difference from core to environment due to lapse rate divergence acting over height H is $\Delta T(LR) = 52℃ - 22℃ = 30℃$.

$\Delta LR = \Delta T(LR)/H = 3℃/\text{km}$ is then the mean lapse rate divergence of the process trace relative to the environmental trace.

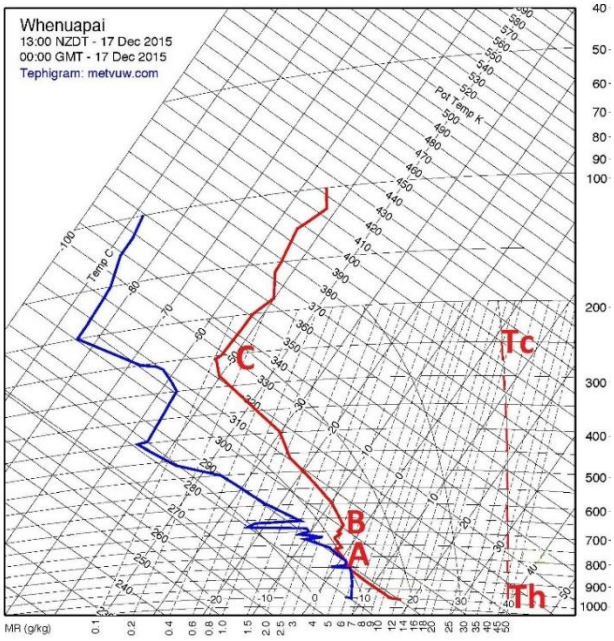

Figure 8. Tephigram of a radiosonde taken at Whenuapai, NZ at 13:00 NZDT on 17th December 2015 (metvuw.com) – mixing ratio [g/kg] on the horizontal axis, pressure [mbar] shown on isobar curves, constant temperatures and potential temperatures shown as sloping lines. The environmental temperature trace is shown in red and dew-point in blue. The core process pseudo-adiabatic trace is shown as a dashed line in red.

4.1 Preliminary Scaling of a Vortex Station

Using equations 1 and 2 and assuming that:

- environmental conditions are as shown in figure 8
- input air to the vortex is raised to $40℃$ and fully saturated, so $T_h = T_0 = 40℃ = 313K$ and $r_0 = 50$ g/kg
- a DVJ structure results with a wind concentration factor of 2 with a wind turbine mounted in the area of maximum flow concentration
- input airflow to the vortex follows the streamline in plan of figure 1b) in a disc of thickness $t = r/6$
- the turbines can extract 50% of the mechanical power of the vortex flows if the extracted power is replaced through additional heating at the Carnot efficiency.
- from the sounding $T_1 = T_\infty = 18℃ = 291K$ and $r_\infty = 6.5$ g/kg
- friction efficiency $\gamma = 95\%$

- temperature of heating is $\overline{T_s} = T_h = 40℃ = 313K$

gives these results:

- Carnot efficiency $\eta = \frac{T_h - T_c}{T_h} = 12\%$
- $V_a = 119$ m/s - a powerful vortex even if compared to a tornado, but not as powerful as given by a cold reservoir at $-50℃$.
- 29MW of available waste heat could be converted to an electrical output of 1.1MW (conversion efficiency 3.9%) in a vortex of 1m core radius, derived from a station with swirl-vanes at 10m radius.

Assuming water is input at 60℃ and cooled by evaporation in the DVJ to 40℃, 29MW represents a flow rate $\dot{V} \approx \rho P_{tot}/(C_w \Delta T) \approx 0.35\ m^3/s$. The required pumping power is $P_p \approx p\dot{V} = 345kPa * 0.35\ m^3/s \approx 120$ kW, based on pressure curves for commercially available dust-suppression nozzles (running at 50psi=345kPa).

A counterintuitive result of this model is that the thermodynamic efficiency of BVP increases if the temperature of the saturated input airflow is reduced, as long as the vortex still rises to the tropopause. The temperature of the cold reservoir falls by more than that of the hot reservoir (assuming the lapse rate divergence is still sufficient for the vortex to rise) as seen in figure 8.

Using the preliminary scaling method given above and varying the temperature of the saturated hot reservoir:

$T_h = 25℃$, $r_0 = 20$ g/kg gives $T_c = -25℃$, $\eta = 17\%$, $V_a = 81$m/s, $\Delta LR = 1.8℃$/km and conversion efficiency is 5.4%

$T_h = 20℃$, $r_0 = 15$ g/kg gives $T_c = -45℃$, $\eta = 21\%$, $V_a = 68$ m/s, $\Delta LR = 0.3℃$/km and conversion efficiency is 6.6%

This suggests a trade-off exists for BVP between conversion efficiency and vortex stability under temperature inversion, depending on the temperature of the saturated input airflow. If lower inflow temperatures are used, then lower feedwater temperatures can also be used, without increased pumping.

A 1MW electrical output would be available from a vortex of approximately 2m core diameter, involving a vortex station of 20m diameter.

The above argument suggests that a conversion efficiency of the order of 5% is achievable in BVP. If existing power station efficiency is 33% and the available waste heat is twice the electrical output, then power station efficiency could be increased by ~10% (from 33% to ~36%) by using such a device.

The two unresolved issues most critical to BVP are:

- The conditions needed for a saturated buoyancy vortex core to rise through a temperature inversion.
- The proportion of the mechanical power in the base of the vortex that can be extracted without destabilizing it.

4.2 Other Models of BVP

Some proponents of BVP [33, 34] analyze the vortex as a heat-engine running to the tropopause and assume that the cold reservoir temperature is the environmental temperature at that height. They derive estimates of cold reservoir temperature around $-80℃$ and consequently high estimates of Carnot efficiency and conversion efficiency. However, there is no evidence that an unsaturated vortex of small diameter will run to the tropopause.

A somewhat different analysis based on CAPE and the total enthalpy supplied to the vortex and assumptions on heat-to-work efficiency based on consideration of Carnot and modified Brayton thermodynamic cycles is given in [4]. Again, the cold reservoir is modeled as having the environmental temperature at the tropopause and estimates of efficiency are higher than our proposed theory would suggest.

5. CONCLUSIONS

The heat engine theory of [10, 11, 32] is used to explain tangential wind velocities occurring in laboratory vortices and dust-devils and statistics of the height of dust devils. We propose the cold reservoir of the heat engine occurs in a turbulent plume, which forms above the vortex core in the absence of adequate lapse rate divergence.

This explains the observed strength of individual dust-devils and points to lapse rate divergence as being necessary to the production of tall, strong buoyancy vortices. In temperate atmospheres, lapse rate divergence is only available from condensation occurring in a saturated vortex core. This implies that buoyancy vortex power generation (BVP) is only plausible using saturated vortices.

The theory is used to scale BVP for the generation of electricity from the waste heat available in secondary cooling water streams at existing thermal power stations, or from low-temperature geothermal resources.

6. REFERENCES

1. Zarrouk SJ, Moon H (2014) Efficiency of geothermal power plants: A worldwide review. *Geothermics 51:142-153*

2. Bardina J, Ferziger JH, Rogallo RS (1985) Effect of rotation on isotropic turbulence: computation and modelling. *Journal of Fluid Mechanics 154:321-336*

3. Zhou Y (1995) A phenomenological treatment of rotating turbulence. *Physics of Fluids (1994-present) 7:2092-2094*

4. Nizetic S (2011) Technical utilisation of convective vortices for carbon-free electricity production: A review. *Energy 36:1236-1242*

5. Ismaeel AA, Al-Kayiem HH, Baheta AT, Aurybi MA (2017) Review and comparative analysis of vortex generation systems for sustainable electric power production. *IET Renewable Power Generation 11:1613-1624*

6. Renno NO, Abreu VJ, Koch J, Smith PH, Hartogensis OK, De Bruin HA, Burose D, Delory GT, Farrell WM, Watts CJ (2004) MATADOR 2002: A pilot field

experiment on convective plumes and dust devils. *Journal of Geophysical Research: Planets (1991–2012) 109*

7. Kanak KM, Lilly DK, Snow JT (2000) The formation of vertical vortices in the convective boundary layer. *Quarterly Journal of the Royal Meteorological Society 126:2789-2810*

8. Klimenko AY (2014) Strong swirl approximation and intensive vortices in the atmosphere. *Journal of Fluid Mechanics 738:268-298*

9. Hess GD, Spillane KT (1990) Characteristics of dust devils in Australia. *Journal of Applied Meteorology 29:498-507*

10. Renno NO, Bluestein HB (2001) A Simple Theory for Waterspouts. *Journal of the Atmospheric Sciences 58:927*

11. Renno N, Burkett M, Larkin MP (1998) A simple thermodynamical theory for dust devils. *Journal of the Atmospheric Sciences 55:3244-3252*

12. Morton BR, Taylor G, Turner JS (1956) Turbulent gravitational convection from maintained and instantaneous sources *Proc. R.Soc. A 234:1-23*

13. Church C, Snow JT, Baker GL, Agee EM (1979) Characteristics of tornado-like vortices as a function of swirl ratio: A laboratory investigation. *Journal of the Atmospheric Sciences 36:1755-1776*

14. Barcilon AI (1967) Vortex decay above a stationary boundary. *Journal of Fluid Mechanics 27:155-175*

15. Renno N (2008) A thermodynamically general theory for convective vortices. *Tellus Series A-Dynamic Meteorology And Oceanography 60:688-699*

16. Mullen JB, Maxworthy T (1977) A laboratory model of dust devil vortices. *Dynamics of Atmospheres and Oceans 1:181-214*

17. Lewellen DC, Lewellen WS, Xia J (2000) The influence of a local swirl ratio on tornado intensification near the surface. *Journal of the Atmospheric Sciences 57:527-544*

18. Lewellen DC, Lewellen WS (2007) Near-surface intensification of tornado vortices. *Journal of the Atmospheric Sciences 64:2176-2194*

19. Rouse H, Yih CS, Humphreys HW (1952) Gravitational convection from a boundary source. *Tellus 4:201-210*

20. Howard LN, Gupta AS (1962) On the hydrodynamic and hydromagnetic stability of swirling flows. *Journal of Fluid Mechanics 14:463-476*

21. Leibovich S, Stewartson K (1983) A sufficient condition for the instability of columnar vortices. *Journal of Fluid Mechanics 126:335-356*

22. Emanuel KA (1984) A note on the stability of columnar vortices. *Journal of Fluid Mechanics 145:235-238*

23. Lewellen WS (1993) Tornado vortex theory. *The Tornado: Its Structure, Dynamics, Prediction, and Hazards: Volume 79 19-39*

24. Kuo HL (1966) On the dynamics of convective atmospheric vortices. *Journal of the Atmospheric Sciences 23:25-42*

25. Ryan JA (1969) Study of Dust Devils as Related to the Martian Yellow Clouds: NASA Report DAC-63098

26. Dergarabedian P, Fendell F (1967) Parameters governing the generation of free vortices. *Physics of Fluids (1958-1988) 10:2293-2299*

27. Yokoyama N, Takaoka M (2017) Hysteretic transitions between quasi-two-dimensional flow and three-dimensional flow in forced rotating turbulence. *Physical Review Fluids 2:092602*

28. Tang Z, Feng C, Wu L, Zuo D, James DL (2017) Characteristics of Tornado-Like Vortices Simulated in a Large-Scale Ward-Type Simulator. *Boundary-Layer Meteorology:1-24*

29. Ryan JA, Carroll JJ (1970) Dust devil wind velocities: Mature state. *Journal of Geophysical Research 75:531-541*

30. Rennó NO, Ingersoll AP (1996) Natural convection as a heat engine: A theory for CAPE. *Journal of the Atmospheric Sciences 53:572-585*

31. Hawkes NA, Flay RGJ (2016) Dust Devil Heights and Windspeeds; *AWES 18, Adelaide*

32. Hawkes NA, Flay RGJ (2017) A Model of Tangential Wind-speeds in Dust-Devils; *APCWE9, Auckland*

33. Michaud LM (2009) The atmospheric vortex engine: *Science and Technology for Humanity: 971-975*

34. Michaud L, Monrad B (2013) Energy from convective vortices: *Applied Mechanics and Materials: 283:73-86*